Design of Robotic System for Cognitive Rehabilitation Based On Computer Vision

Article *in* Journal of Engineering and Science in Medical Diagnostics and Therapy · February 2020

DOI: 10.1115/1.4046396

4 authors:

Haodong Chen
University of Maryland, College Park
22 PUBLICATIONS **139** CITATIONS
SEE PROFILE

Hongbo Zhu
Columbia University
1 PUBLICATION **5** CITATIONS
SEE PROFILE

Zhiqiang Teng
Heifei University of Technology
5 PUBLICATIONS **17** CITATIONS
SEE PROFILE

Ping Zhao
Hefei University of Technology
41 PUBLICATIONS **334** CITATIONS
SEE PROFILE

Design of a Robotic Rehabilitation System for Mild Cognitive Impairment Based on Computer Vision

Hao-dong Chen
School of Mechanical Engineering,
Hefei University of Technology,
Hefei, Anhui 230009, China;
Department of Mechanical
Engineering and Aeraspace,
Missouri University of Science and Technology,
Rolla, MO 65409

Hongbo Zhu
Department of Mechanical Engineering,
Columbia University,
New York, NY 10027

Zhiqiang Teng
School of Mechanical Engineering,
Hefei University of Technology,
Hefei, Anhui 230009, China

Ping Zhao[1]
School of Mechanical Engineering,
Hefei University of Technology,
Hefei, Anhui 230009, China
e-mail: ping.zhao@hfut.edu.cn

This paper develops a robotic cognitive rehabilitation therapy (CRT) system to assist patients with mild cognitive impairment (MCI) in block design test (BDT) rehabilitation training. This system bridges the treatment gap that occurs when one physician has several patients to attend to. One physician can setup the BDT training task and simultaneously monitor the training progress of several patients with MCI, which forms an effective one-to-many rehabilitation model. A target information acquisition method is designed to realize target detection and position extraction in automatic rehabilitation. Two graphic user interfaces (GUIs) are developed to provide intuitive control and immediate visual feedback. Different BDTs are selected from the benchmark by the physician in an integrated GUI (I-GUI) and are assigned to several patient GUIs (P-GUIs), respectively. During training, automatic visual assistance can be triggered by the help button and the patients can be guided in finding the target block. Additionally, a robotic arm could be engaged to further help with teaching so that patients can follow the instructions given by the P-GUI and imitate the demonstration given by the robot arm to finish the training task. This system converts traditional MCI rehabilitation into an automatic process, creating an effective model of BDT training for MCI rehabilitation.
[DOI: 10.1115/1.4046396]

Keywords: mild cognitive impairment (MCI), cognitive rehabilitation, block design test (BDT), robotic system, graphic user interface (GUI)

1 Introduction

Cognitive impairment is a defining feature of Alzheimer's disease and is a common symptom of many other neurodegenerative conditions. Patients with cognitive impairment suffer with substantial pain. Additionally, patients with mild cognitive impairment (MCI) have a higher risk of subsequently developing dementia [1]. With advancements in modern science, the detection rate of early MCI has increased drastically. To obtain a better cognitive assessment, several related strategies have been designed. In 1938, Raven's standard progressive matrices were published in the United Kingdom. This assessment consists of a 60-item test used in measuring abstract reasoning and is regarded as a nonverbal estimate of fluid intelligence [2]. Later, in 1955, the Wechsler adult intelligence scale (WAIS) was proposed by David Wechsler. It is an intelligence quotient test designed to measure intelligence and cognitive ability in adults and older adolescents [3,4]. In 2005, the Montreal cognitive assessment (MoCA), an accurate method proposed by Nasreddine, was widely used to test the condition of cognitive disorder patients [5]. At the Alzheimer's Association International Conference 2016 (AAIC2016), a 38-point checklist was proposed by Ismail that could help doctors identify behavioral changes in patients and measure their progress over time [6]. Furthermore, many cognitive training methods have been proposed as effective ways to assist in the rehabilitation of patients with MCI. In 1981, one WAIS-R test, the block design test (BDT), was proposed by Wechsler. This test is thought to reflect visuospatial constructional ability [7] and is a reasonably good predictor of everyday spatial measures [8]. Then, the BDT began to be widely utilized in the field of cognitive rehabilitation therapy (CRT). In 2004, a spatial tangible user interface for cognitive assessment and training was proposed by Ehud Sharlin and Yuichi Itoh, and cognitive cubes were applied in this technology [9]. Two slightly modified versions of the BDT were used by Caron et al. in a method called CBDT, which could assess visual constructive and perceptual skills by using configurations with high or low levels of cohesiveness and task uncertainty, respectively [10]. In 2017, BDT and BBDT were applied in children with dyslexia or other nonverbal learning disabilities [11]. These methods, to a certain extent, improve the cognitive ability of patients. However, the coverage of rehabilitation services and medical human resources are not adequate. Training is often too fragmented, uncoordinated, and unresponsive to the needs of people living with dementia [12].

To improve automatic assistance in the field of rehabilitation, the development of robot assistant rehabilitation is popular. With the assistance of robots, the burden of caregivers has the potential to be diminished [13]. In 2012, a CRT robot was developed for unilateral spatial neglect patients by Kubota et al. Based on 3D distance image sensors, this robot could observe human motions. The observed data could provide important information for the therapist to indicate the state of rehabilitation [14]. In the same year, another cognitive training robot was proposed by Chan et al. This human-like robot engaged individuals in person-centered cognitively stimulating activities and could provide assistance, encouragement, and celebration during the course of an activity

[1]Corresponding author.

Contributed by the Applied Mechanics Division Technical Committee on Dynamics & Control of Structures & Systems (AMD-DCSS) of ASME for publication in the Journal of Engineering and Science in Medical Diagnostics and Therapy. Manuscript received October 17, 2019; final manuscript received February 17, 2020; published online March 11, 2020. Assoc. Editor: Ning An.

Table 1 Tasks grouped by index in WAIS-IV

Index	Verbal comprehension	Working memory	Processing speed	Perceptual reasoning
Task	Similarities Vocabulary Information Comprehension	Digit span Arithmetic Letter-number Sequencing	Symbol search Coding Cancellation	Block design Matrix reasoning Visual puzzles Picture completion Figure weights

[15]. In 2014, Rudzicz et al. developed a mobile robotic platform, which intended to be used as a personal caregiver to help with the performance of activities of daily living. This robot is based on speech recognition technology [16]. In 2018, Antonio Andriella et al. developed a decision system to embed in a robot that could setup a productive interaction with an Alzheimer's disease or an MCI patient and could be employed by the caregiver to motivate and support patients while performing cognitive exercises [17].

In this paper, a robotic CRT system is designed based on WAIS-IV and BDT. The scale is currently in its fourth edition (WAIS-IV), which was released in 2008 by Pearson (data collection for the next version (WAIS V) began in 2016 and is projected to be complete in 2019). This scale is an important practical and clinical diagnostic tool and is also indispensable in the scientific study of cognitive brain functions. The four index and related tasks of WAIS-IV are shown in Table 1. BDT is one task measuring perceptual reasoning and is popular in MCI rehabilitation [18]. Generally, the blocks in the BDT are in the same color. However, in this system, a modified visual-constructive version is adopted, involving the recognition, transformation, and construction of blocks of different types of color. The proposed abilities of patients measured during the modified BDT task are visual motor construction, visual spatial processing, problem solving, and quick perception of visual details [19].

The rehabilitation system proposed in this study addresses two main issues: physician control and patient rehabilitation. With this system, physicians and caregivers are able to manage the rehabilitation BDT for more than one patient, i.e., the one-to-many model. In terms of patient rehabilitation, with the highlighted hints of BDT outputs on the screen and the robotic demonstration, the rehabilitation process is almost the same as that in the regular BDT process. In the development of the assistance method, to highlight hints for specific blocks in the workspace, classification based on Fourier descriptors (FDs) and normalization are adopted for target detection, and an image matching method is proposed for the extraction of position information. Kinematics control of a six degrees-of-freedom robotic arm is conducted in the robotic demonstration.

This organization of the paper is as follows. Section 2 illustrates a set of algorithms and methods designed for the system and the construction of a whole robotic CRT system. Section 3 demonstrates the implementation strategy of the system in the BDT for MCI rehabilitation. Experiments with the system are implemented in Sec. 4. The results show the merits of the robotic CRT system as a creative and timesaving method for cognitive rehabilitation.

2 Construction of the Rehabilitation System

In this section, we adopt FDs algorithm [20] in the visual task for target detection and propose the modulus-shift matching (MSM) algorithm in the image matching process [21,22]. Then, two different but interrelated GUI software programs are designed. Furthermore, the one-to-many rehabilitation model is realized in the construction of the rehabilitation system.

2.1 Target Acquisition Algorithm in the Rehabilitation System. After obtaining an image of the workspace with cameras, preprocessing is first implemented. Each pixel gray value is set to the median value of all pixel values in the neighborhood of the point, and the grayscale images are obtained. Then, binary images are extracted after binarization processing. The opening–closing operation is applied to binary images to realize noise removal. The opening operation removes small objects from the foreground, placing them in the background, while the closing operation removes small holes in the foreground, changing small islands of the background into foreground [23]. Then, the holes of the parts are eliminated. Each part includes one connected domain. After that, the Gaussian convolutions adopted remove noise. Based on the Canny operator, image contours are extracted [24]. The equation generating a Gaussian filter kernel with a size of $(2k+1)\times(2k+1)$ is shown as follows:

$$H_{ij}=\frac{1}{2\pi\sigma^2}\exp\left\{-\frac{[i-(k+1)]^2+[j-(k+1)]^2}{2\sigma^2}\right\};\quad 1\le i,j\le 2k+1 \tag{1}$$

where σ is the variance, and $2k+1$ is the dimension of kernel matrix.

The horizontal, vertical, and diagonal edges in the image are detected, and the first derivative values in the horizontal component Gx and vertical component Gy directions are returned, from which the gradient G and the angle θ of the pixel can be determined as the following equation:

$$G=\sqrt{G_x^2+G_y^2}\qquad \theta=\arctan\left(\frac{G_y}{G_y}\right) \tag{2}$$

Based on nonmaximum suppression, all gradient values that equal zero except the local maximum are suppressed. The maximums are determined as accurate edges, and the remaining pixel is represented by Gp. The edges obtained previously are connected based on a double threshold algorithm. A high threshold and a low threshold should be considered in this step. The contour decision strategy of pixels is shown in Table 2.

The previously mentioned strong edge will be regarded as a real contour. However, the weak edge will also be regarded as a real edge only if this pixel is connected to at least one strong edge in eight neighborhood directions. Generally, the high threshold and the low threshold of the Canny edge detection are set based on the gray scale image. With the adoption of the Otsu's method, this threshold is determined by minimizing intraclass intensity variance, or equivalently, by maximizing interclass variance [24].

Since the contours are obtained, the target detection based on FD classification is conducted, i.e., finding the objects constructing the target structure. As shown in Fig. 1, with the adoption of

Table 2 Decision strategy of edge extraction

Condition	Decision
Gp ≥ high threshold	Strong contour
Gp < low threshold	Suppression
High threshold > Gp ≥ Low threshold	Weak coutour

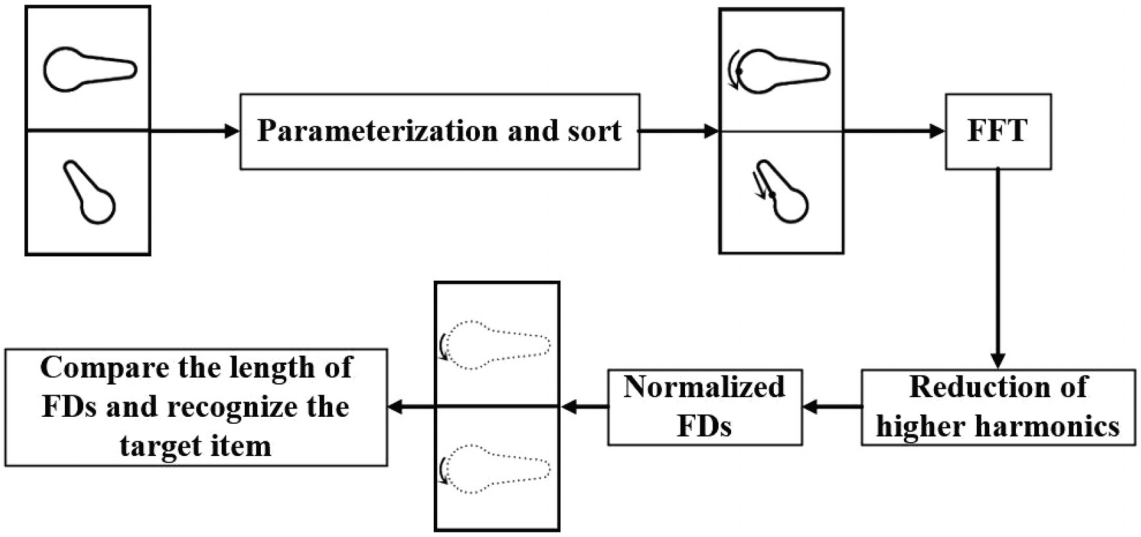

Fig. 1 Demonstration of FDs algorithm

Table 3 Normalized FDs

Geometric invariance	Operation in normalized FDs
Translation	$F(0) = 0$
Scale	$F(k) = \dfrac{F(k)}{\|\|F(1)\|\|},\ k = 0, 1, \ldots, N-1;$
Rotation and starting point	$F(k) = \|\|F(k)\|\|,\ k = 0, 1, \ldots, N-1$

Fourier descriptors, the discrete-time periodic signals of the initial image contours are mapped to the frequency domain

$$F(k) = \sum_{n=0}^{N-1} Z_n e^{\frac{-j2\pi kn}{N}}, \quad 0 \le k \le N-1 \tag{3}$$

where k denotes the index of FDs.

In the above-mentioned expression, all the geometric information, including translation, rotation, scale, and starting point, is combined. Since the translation information is only contained in the zero order of FDs, it is set as zero. Then, the scale factor exists in all magnitudes of the FDs and could be eliminated after dividing by the first order. Additionally, the rotation and starting point can be reflected by the phase angle of each harmonic component, which can be eliminated by using only the magnitude of $F(k)$. With implement of normalized FDs shown in Table 3, the effect of translation, scale, rotation, and choice of starting point can be eliminated [25]. By comparing the least square error of the non-zero parameters in the FDs between the prescribed shapes and actual image contour in the workspace, the actual targets can be recognized. Figures 2(*a*)–2(*d*) performance and results of the FD algorithm. Figure 2(*d*) shows that identified targets (a) and (b) are colored in, while others are included as obstacles.

After target detection, to acquire the rotation angle between the reference contour and the target contour in the workspace, the MSM algorithm is designed to calculate the phase information. First, we convert the coordinates of two identical contours with different rotation angles to polar space and obtain the phase angles of all contour points. Then, the points are sorted by the phase angle, and the amount of the points is adjusted to be equal. Next, two series of complex numbers are obtained. To determine the rotation angle between these two similar shapes, take an arbitrary rotational transformation on one shape and compute the least square error between two series of complex numbers, and then, find the optimal rotational transformation that could minimize this error. Note that in this process, only the modulus part of each complex number is shifted, but the phase part (i.e., the angle) remains, which combines into a brand new series of complex numbers, as shown in Fig. 3. In Fig. 3, after representing contours (a) and (b) in polar coordinates, we obtain the modulus of the contour points and plot them in Fig. 3(*c*). The shifting and matching process is then conducted, and the angles of the rotation that minimizes the errors between (a) and (b) are found as shown in Fig. 3(*d*). The pseudo-code of this algorithm is shown in Algorithm 1. The rotation angle obtained will be adopted in the demonstration by robotic arm.

To show the feasibility of the MSM algorithm, a group of tests are conducted (Fig. 4). The position detection results are presented in Table 4. It could be observed that the error in the angle of rotation is less than 2 deg. Structural design in the assembly process, such as a guiding slot, could compensate for such a small error. With such acceptable accuracy, adopting the MSM algorithm could successfully determine the position of the target machine parts despite the starting point choice.

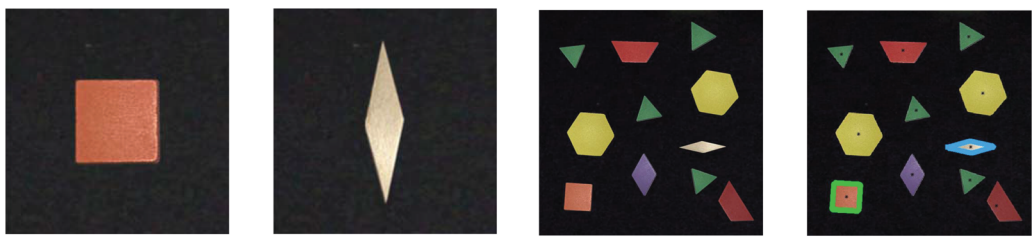

(*a*) (*b*) (*c*) (*d*)

Fig. 2 The performance of target detection based on FDs

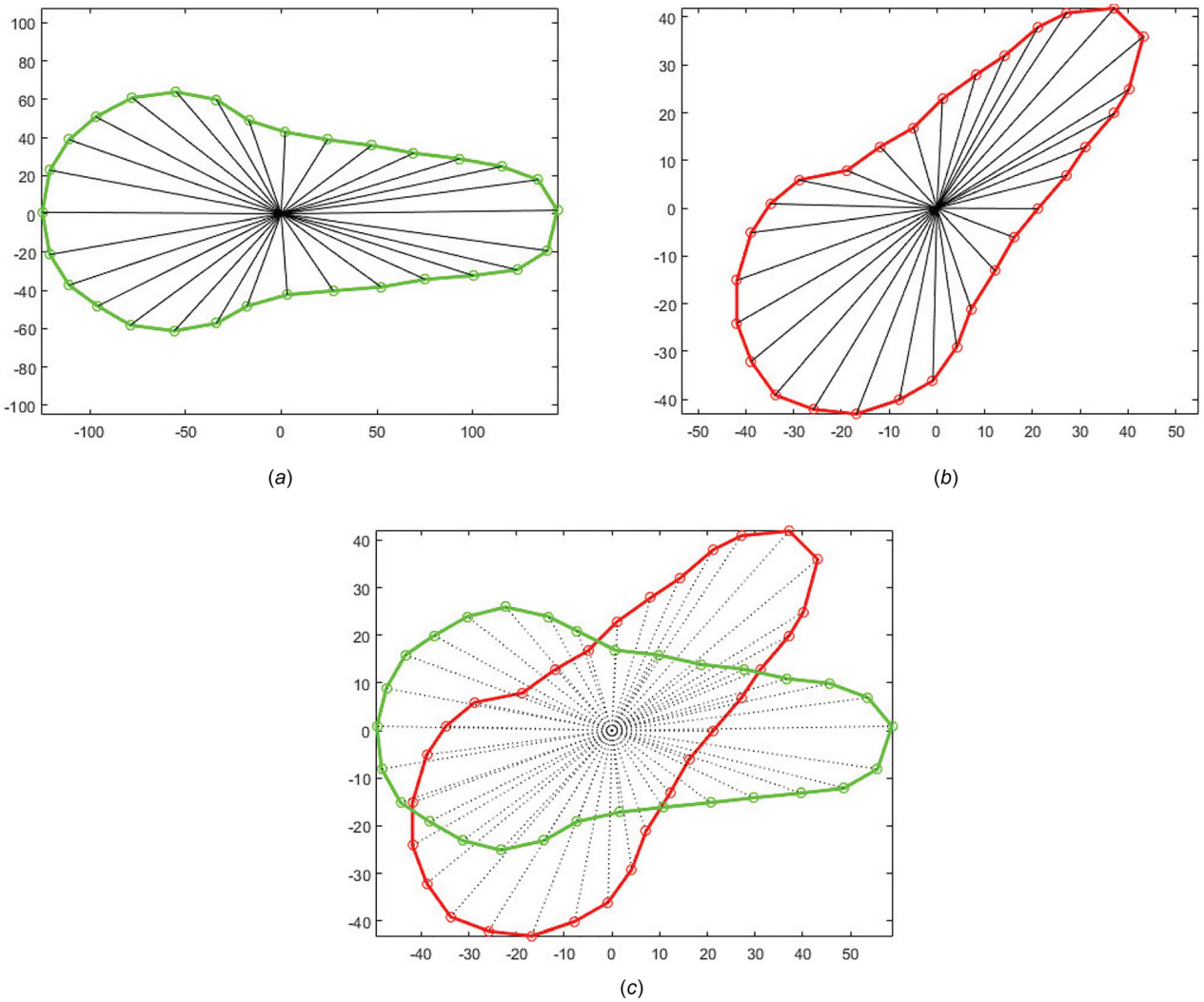

Fig. 3 Illustration of MSM algorithm

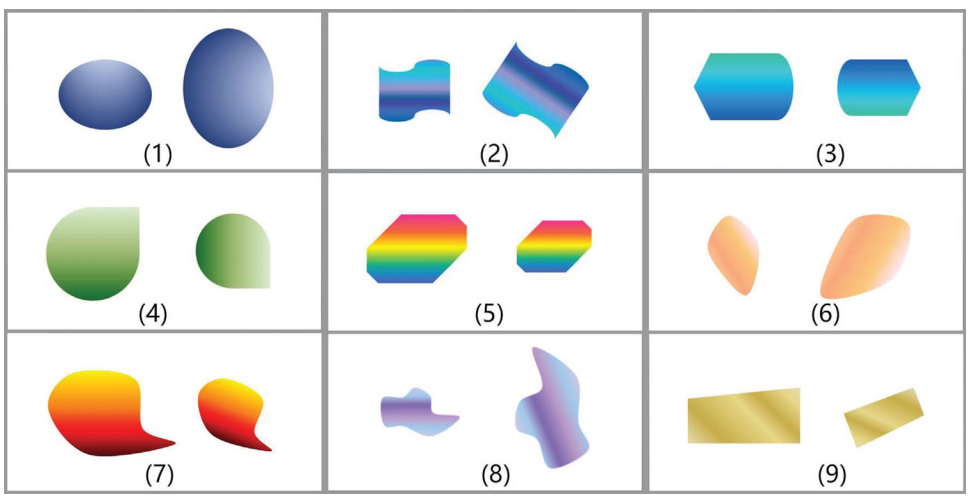

Fig. 4 Group of MSM algorithm tests with given shapes

Table 4 Prescribed rotational angles in Fig. 5 and the resulting angles from our MSM algorithm

Order	Prescribed	Results	Error
1	90.00 deg	88.30 deg	1.70 deg
2	22.00 deg	21.44 deg	0.56 deg
3	90.00 deg	90.49 deg	0.49 deg
4	214.00 deg	215.27 deg	1.27 deg
5	0.00 deg	359.27 deg	0.73 deg
6	248.00 deg	249.12 deg	1.12 deg
7	270.00 deg	268.73 deg	1.27 deg
8	63.00 deg	63.84 deg	0.84 deg
9	160 deg	161.53 deg	1.53 deg

Algorithm 1 Modulus-Shift Matching

Input: Ur(Mr, Ar), Ut(Mt, At)/* two sets of modulus and phase angles matrixes of reference and target edge points*/

Output: Rotational angle and scale of two edges;

1: **function** MODULUS-SHIFT MATCHING (Ur(Mr, Ar), Ut(Mt, At))
2: Resize the amount of points of Ur and Ut to be equal;
3: Num ← number of Ut;
4: **for** each $i \in [1, \text{Num}]$ **do**
5: $\text{Mt} \leftarrow [\text{Mt}(2:\text{Num}), \text{Mt}(1)]$
6: $\text{diff}(i) \leftarrow \sum_{i=1}^{\text{Num}} |\text{Mt}(i) - \text{Mt}(i)|$
7: threshold ← defined by the size of image;
8: **if** $\text{diff}(i) < \text{threshold}$ **then**
9: mindiff ← i/*record the position of the minimum difference*/
10: threshold ← $\text{diff}(i)$/*update the threshold*/
11: **end if**
12: **end for**
13: $\text{Angle} \leftarrow (\text{At}(\text{mindiff}) - \text{At}(1))/\pi * 180$;
14: $\text{Scale} \leftarrow \text{Sum}(\text{Mr})/\text{Sum}(\text{Mt})$
15: **end function**

2.2 Design of the Graphic User Interfaces. In the graphic user interface (GUI) design stage, two different designs are designed for physicians and patients. As shown in Fig. 5(*a*), the integrated GUI (I-GUI) for physicians includes four kinds of button groups and an interface window. With the task button, physicians can select a specific BDT from a benchmark consisting of different kinds of tasks. With patient buttons and a camera button, physicians can monitor the rehabilitation progress of more than one patient at any time, and the progress will be obtained by the camera and shown on the window. Note that in the future, with more patient buttons, one physician would be able to assist more patients to realize the one-to-many model. In addition, there are also function buttons that are designed to stop the rehabilitation process, clear the window, and save the patient data related to the rehabilitation results. The patient GUI (P-GUI), shown in Fig. 5(*b*), is much more intuitive and much clearer. There is only one help button and an interface window. Patients can obtain the help they need from the system by the direct manipulation of this GUI, as mentioned earlier, and the assistance includes a highlighted hint and a robotic demonstration.

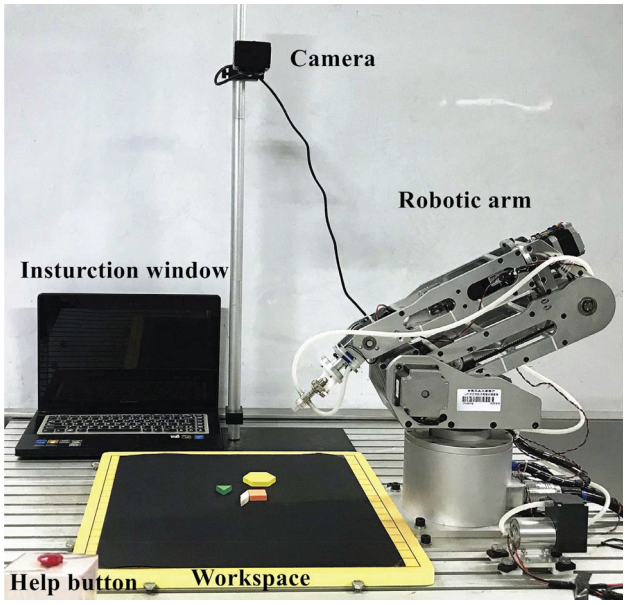

Fig. 6 Construction of the whole rehabilitation system

2.3 Construction of the Rehabilitation System. Figure 6 shows the cognitive rehabilitation system, including a camera, a six degrees-of-freedom robotic arm, an instruction window, a workspace, and a help button. The camera is fixed above the workspace and thus can monitor the whole workspace and obtain images as the input of the system. The instruction window on the left is used to show the P-GUI to patients and guide them. Blocks in the workspace constituting the BDT need to be finished in the CRT. The robotic arm on the right has six degrees-of-freedom derived by six motors produced by SAMSR company, Japan. The help button on the left is red, sharing the same function as the help button in the P-GUI. By pushing the button, patients can

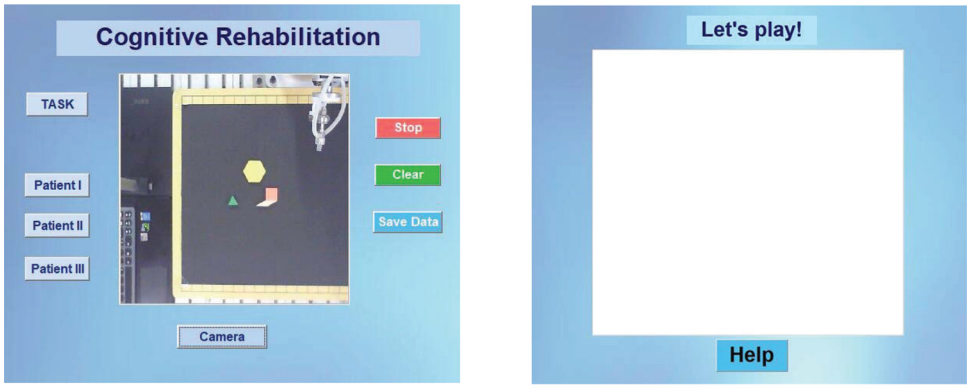

(*a*) (*b*)

Fig. 5 The P-GUI for physician and the I-GUI for patient

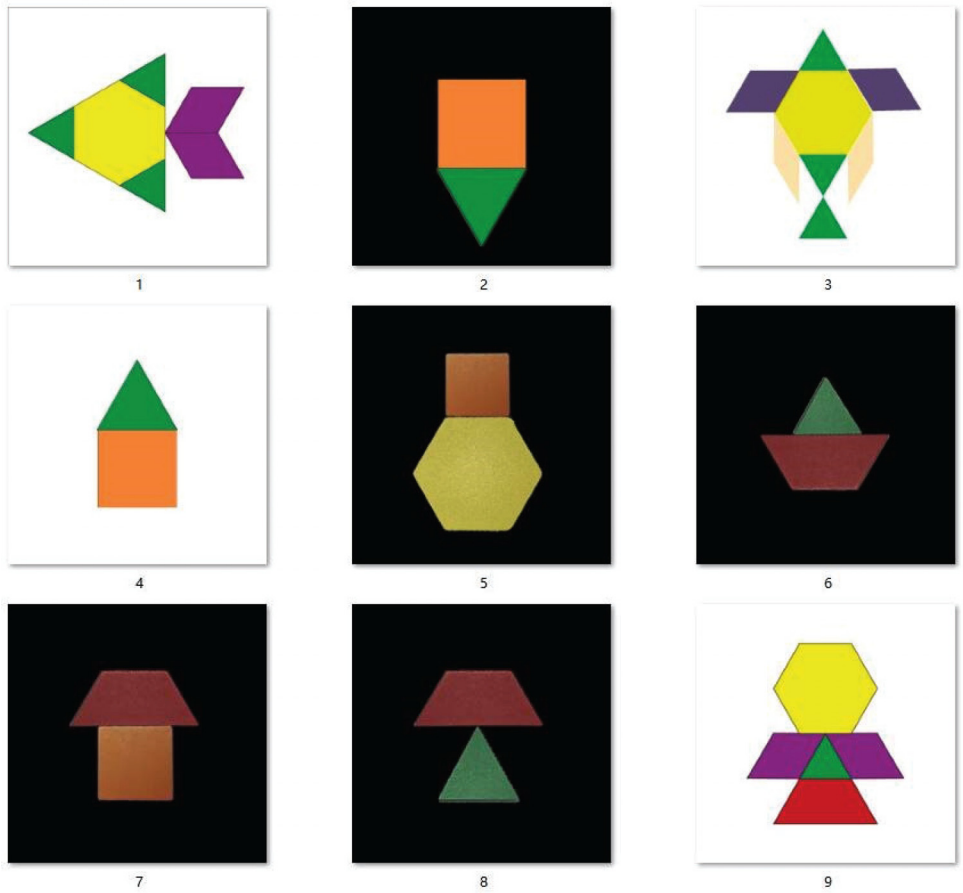

Fig. 7 Benchmark of the BDT

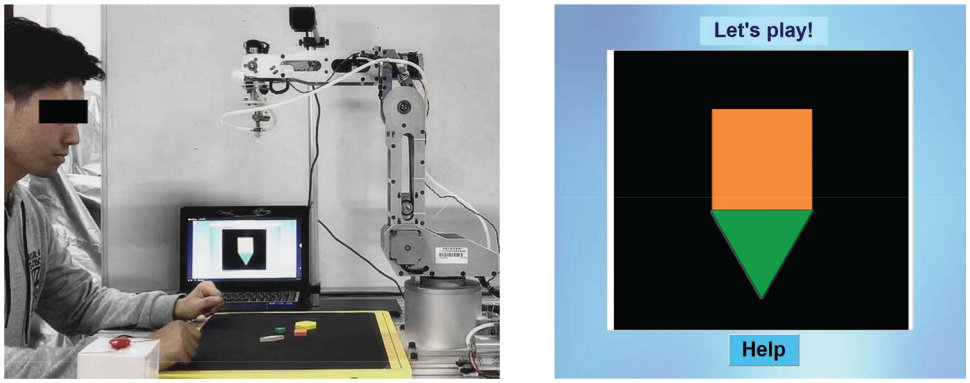

(*a*) (*b*)

Fig. 8 Specific task of rehabilitation for the SP: (*a*) side view and (*b*) instruction window

obtain the help they need easily. The control device includes the computer and the six-axis controller. The controller ID is YJ-CTRL-A601.

3 Implementation Stretchy of the Rehabilitation System

In the implementation of the rehabilitation system, one effective and highly individualized rehabilitation method is developed. First, the training task can be defined by a physician in the I-GUI, and different kinds of tasks are designed and documented in the benchmark. Then, the training process in the platform can be obtained by camera. Based on the FD method, the target blocks that need to be moved in the specific task will be highlighted and shown on the P-GUI window, which can instruct the patients to distinguish blocks with different poses and colors and find the blocks used in the construction of the target shape. If the patient cannot understand the hint and finish the task, the robotic arm will conduct a demonstration on the platform to teach the patient how to finish the task; the function of this part of the system is similar to that of the assistance of a physician beside the patient, but with higher accuracy and efficiency. In this way, the patient can learn and imitate the movement of the robot arm to finish the training task.

4 Experiment

In this section, we presented an experiment to a simulated patient (SP) to demonstrate the operation mode and functions of

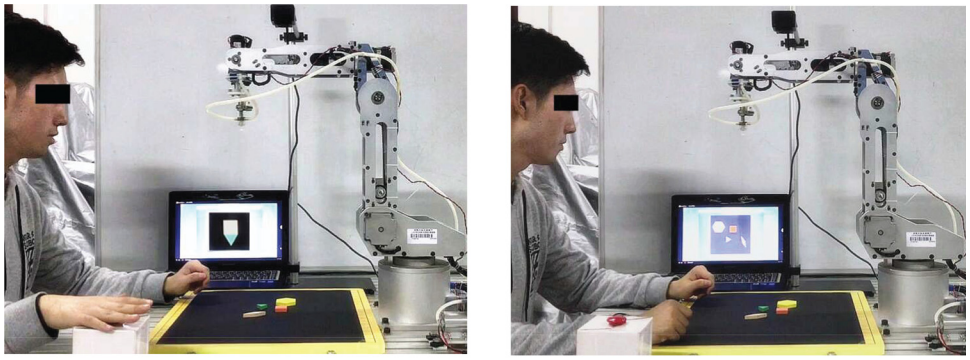

(*a*) (*b*)

Fig. 9 The side view of help button and highlighted blocks in the workspace for the SP: (*a*) help button and (*b*) highlight

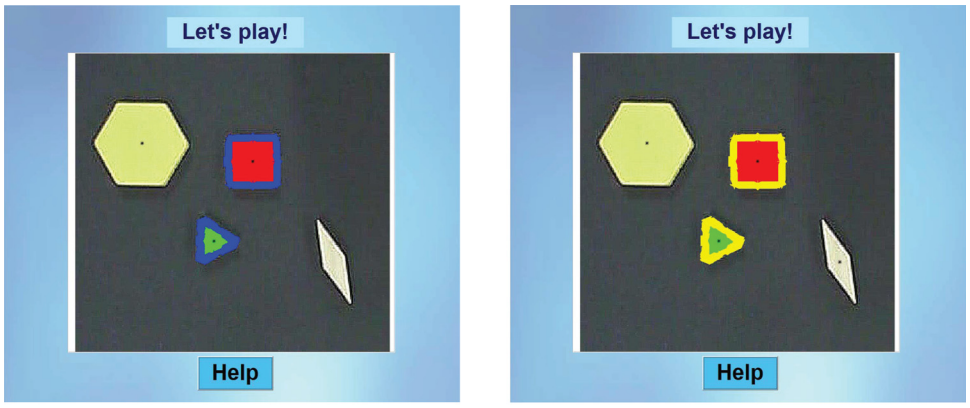

(*a*) (*b*)

Fig. 10 The highlighted hint in the P-GUI for the SP

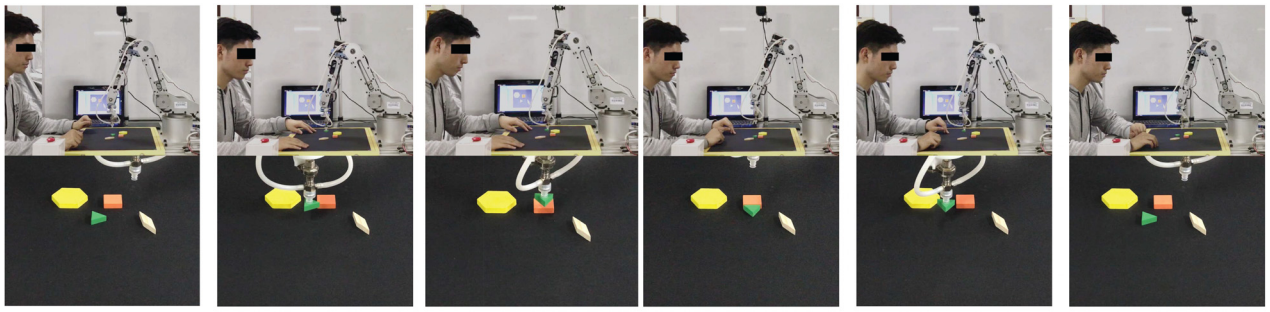

(*a*) (*b*) (*c*) (*d*) (*e*) (*f*)

Fig. 11 The robotic demonstration process of CRT

the rehabilitation system for the BDT rehabilitation training of patients with MCI.

4.1 Experiment Process. There are six main steps in the rehabilitation system.

Step 1: As shown in Fig. 7, with the task button of the I-GUI, a predesigned BDT benchmark is shown. The physician can select a different BDT for each patient and can also monitor the patients (Fig. 5(*a*)).

Step 2: As shown in Fig. 8(*b*), the robot arm is in the initial pose. Here, the rehabilitation process of the subject (simulated patient) will be illustrated. The patient is positioned on the left side of the system, in front of the workspace. Since the physician has selected a specific task for him, this task is shown in the instruction window. The task stimulus is a simple BDT shape consisting of an orange square block and a green triangle block.

Step 3: During the BDT construction, if patient has difficulty, as shown in Fig. 9(*a*), by pushing the "help" button beside his right hand, the workspace captured by camera will be input into the system. With the related target acquisition algorithm in Sec. 2, the target blocks in the workspace, i.e., the orange square and green triangle, are detected and colored red and green in the workspace picture(as shown in Figs. 10(*a*) and 10(*b*)). The edges of the blocks alternately flash blue and yellow to help patients better and more easily recognize them. This step just simulates the prime help given by physicians in general BDT rehabilitation, pointing out the target blocks and giving patients a hint. In this system, it is

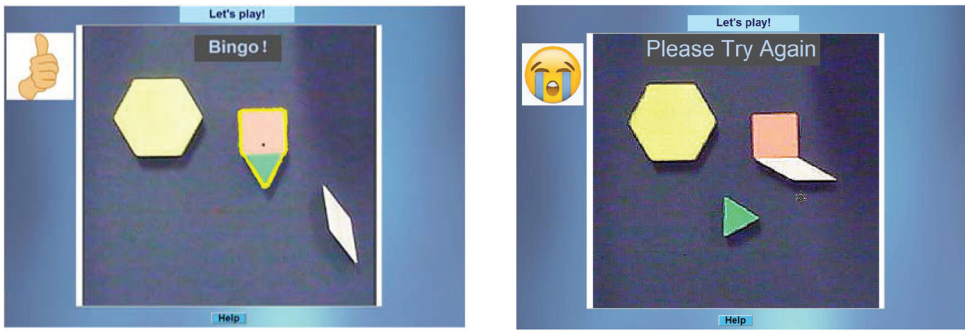

(*a*) (*b*)

Fig. 12 The results of BDT training for SP I: (*a*) correct and (*b*) wrong

much more intuitively clear. With this assistance, some MCI patients, especially in the early stage of MCI, might be able to overcome cognitive impairment and continue the task.

Step 4: In actual rehabilitation, when patients do not understand the logic of the physician's hint, the physician will teach them by demonstrating how to finish the task. Patients can watch and imitate the demonstration to accomplish the task. In our rehabilitation system, during similar situations, patients can push the help button again to start the robotic demonstration program. Based on the target acquisition algorithm, i.e., the FDs, the MSM algorithm and kinematics control, the robotic arm will begin to teach patient how to finish this task. In the experiment, first, the green triangle block was sucked by the sucker, i.e., the end effector of the robotic arm (Figs. 11(*a*) and 11(*b*)). Then, in Figs. 11(*c*) and 11(*d*)), the block was delivered to a specific location in the same position as the target shape in Fig. 8. The patient could also observe this demonstration process. At the end, the green triangle block will be moved back to the original location in the initial position (Figs. 11(*e*)–11(*f*)). This demonstration imitates the function of physicians in teaching patients with BDT. Furthermore, during the entire process, the highlighted image in the workspace remains on the P-GUI window. Therefore, the patient can obtain the help he needs at any time during rehabilitation.

4.2 Experimental Results. After learning from the instruction window and the demonstration of the robotic arm, the patient can be led to understand the right procedures needed to finish the task. During the rehabilitation process in the task, the conditions of every workspace can be monitored by a physician. Additionally, the system will detect the results of all patients automatically. As shown in Fig. 12(*a*), the SP is encouraged after he finishes the BDT task successfully. If he does not complete the BDT task successfully, he would be encouraged to try again, and the system would repeat the above-mentioned assistance process.

5 Conclusions

The main purpose of this study is to develop a robotic CRT system for MCI patients and realize automatic instruction and assistance in BDT training. A one-to-many model based on two GUI software programs and computer vision is designed. A series of target detection and position extraction algorithms that are compatible with this system are designed. Two methods are used in the assistance process to satisfy necessary guidance in the rehabilitation training. The initial step is to highlight specific target blocks in the workspace image. A more advanced step is to start the robotic arm to help teach the task. With this system, several simultaneous BDT rehabilitation sessions for different patients can be simultaneously realized and controlled by only one physician. In the application experiment, the system can function accurately and conveniently as an assistant. The time the system saves and the guidance it gives substantially benefit both medical staff and patients. One of the main contributions of this rehabilitation system are that patients can obtain more accurate guidance and assistance and more positive encouragement and celebration during rehabilitation; in addition, the creative one-to-many model alleviates pressure from having limited medical human resources and effectively assists physicians in BDT rehabilitation of patients with MCI.

Acknowledgment

All findings and results presented in this paper are those of the authors and do not represent those of the funding agencies.

Funding Data

- National Natural Science Foundation of China (Ping Zhao, Project No. 51775155; Funder ID: 10.13039/501100001809).
- Anhui Provincial Key R&D Project (Ping Zhao, No. 201904b11020035; Funder ID: 10.13039/501100003995).

References

[1] Jelic, V., Kivipelto, M., and Winblad, B., 2006, "Clinical Trials in Mild Cognitive Impairment: Lessons for the Future," J. Neurol., Neurosurg. Psychiatry, **77**(4), pp. 429–438.
[2] Qiu, F., Wei, Q., Zhao, L., and Lin, L., 2009, "Study on Improving Fluid Intelligence Through Cognitive Training System Based on Gabor Stimulus," First International Conference on Information Science and Engineering, Nanjing, China, Dec. 26–28, pp. 3459–3462.
[3] Bright, P., Hale, E., Gooch, V. J., Myhill, T., and van der Linde, I., 2018, "The National Adult Reading Test: Restandardisation Against the Wechsler Adult Intelligence Scale-Fourth Edition," Neuropsychol. Rehabil., **28**(6), pp. 1019–1027.
[4] Pangman, V. C., Sloan, J., and Guse, L., 2000, "An Examination of Psychometric Properties of the Mini-Mental State Examination and the Standardized Mini-Mental State Examination: Implications for Clinical Practice," Appl. Nurs. Res., **13**(4), pp. 209–213.
[5] Nasreddine, Z. S., Phillips, N. A., BÃ©Dirian, VÃ©R., Charbonneau, S., Whitehead, V., Collin, I., Cummings, J. L., and Chertkow, H., 2005, "The Montreal Cognitive Assessment, Moca: A Brief Screening Tool for Mild Cognitive Impairment," J. Am. Geriatr. Soc., **53**(4), pp. 695–699.
[6] Mallo, S. C., Ismail, Z., Pereiro, A. X., Facal, D., Lojo-Seoane, C., Campos-Magdaleno, M., and Juncos-Rabadán, O., 2019, "Assessing Mild Behavioral Impairment With the Mild Behavioral Impairment Checklist in People With Subjective Cognitive Decline," Int. Psychogeriatr., **31**(2), pp. 231–239.
[7] Kaufman, A. S., 1983, "Test Review: Wechsler, D. Manual for the Wechsler Adult Intelligence Scale, Revised. New York: Psychological Corporation, 1981," J. Psychoeduc. Assess., **1**(3), pp. 309–313.
[8] Groth-Marnat, G., and Teal, M., 2000, "Block Design as a Measure of Everyday Spatial Ability: A Study of Ecological Validity," Perceptual Motor Skills, **90**(2), pp. 522–526.
[9] Sharlin, E., Itoh, Y., Watson, B., Kitamura, Y., Sutphen, S., Liu, L., and Kishino, F., 2004, "Spatial Tangible User Interfaces for Cognitive Assessment and Training," International Workshop on Biologically Inspired Approaches to Advanced Information Technology, Lausanne, Switzerland, Jan. 29–30, pp. 137–152.
[10] Caron, M.-J., Mottron, L., Berthiaume, C., and Dawson, M., 2006, "Cognitive Mechanisms, Specificity and Neural Underpinnings of Visuospatial Peaks in Autism," Brain, **129**(7), pp. 1789–1802.
[11] Cardillo, R., Mammarella, I. C., Garcia, R. B., and Cornoldi, C., 2017, "Local and Global Processing in Block Design Tasks in Children With Dyslexia or Nonverbal Learning Disability," Res. Dev. Disabil., **64**, pp. 96–107.

[12] Kanno, K. M., Lamounier, E. A., Cardoso, A., Lopes, E. J., and de Lima, G. F. M., 2018, "Augmented Reality System for Aiding Mild Alzheimer Patients and Caregivers," IEEE Conference on Virtual Reality and 3D User Interfaces (VR), Reutlingen, Germany, Mar. 18–22, pp. 593–594.
[13] Cristina Nascimento Dourado, M., and Laks, J., 2016, "Psychological Interventions for Neuropsychiatric Disturbances in Mild and Moderate Alzheimer's Disease: Current Evidences and Future Directions," Curr. Alzheimer Res., **13**(10), pp. 1100–1111.
[14] Kubota, N., Botzheim, J., and Obo, T., 2012, "Human Motion Tracking and Feature Extraction for Cognitive Rehabilitation in Informationally Structured Space," Ninth France-Japan and Seventh Europe-Asia Congress on Mechatronics (MECATRONICS)/13th International Workshop on Research and Education in Mechatronics (REM), Paris, France, Nov. 21–23, pp. 464–471.
[15] Chan, J., and Nejat, G., 2012, "Social Intelligence for a Robot Engaging People in Cognitive Training Activities," Int. J. Adv. Rob. Syst., **9**(4), p. 113.
[16] Rudzicz, F., Wang, R., Begum, M., and Mihailidis, A., 2014, "Speech Recognition in Alzheimer's Disease With Personal Assistive Robots," Proceedings of the Fifth Workshop on Speech and Language Processing for Assistive Technologies, Baltimore, MD, June, pp. 20–28.
[17] Andriella, A., Alenyà, G., Hernández-Farigola, J., and Torras, C., 2018, "Deciding the Different Robot Roles for Patient Cognitive Training," Int. J. Human-Comput. Stud., **117**, pp. 20–29.
[18] Serbin, L. A., and Connor, J. M., 1979, "Sex-Typing of Children's Play Preferences and Patterns of Cognitive Performance," J. Genetic Psychol., **134**(2), pp. 315–316.
[19] Drozdick, L. W., Wahlstrom, D., Zhu, J., and Weiss, L. G., 2012, "The Wechsler Adult Intelligence Scale-Fourth Edition and the Wechsler Memory Scale," 4th edition, Contemporary Intellectual Assessment: Theories, Tests, and Issues, The Guilford Press, New York, pp. 197–223.
[20] Zhu, H. G., and Feng, Q., 2013, "A Video Bit Rate Control Algorithm Based on Weighted Estimate of Image Brightness Difference," Appl. Mech. Mater., **347**, pp. 844–848.
[21] Chen, H.-D., Wang, Y.-F., Guo, Z., Chen, W.-X., and Zhao, P., 2018, "A GUI Software for Automatic Assembly Based on Machine Vision," IEEE International Conference on Mechatronics, Robotics and Automation (ICMRA), Hefei, China, May 18–21, pp. 105–111.
[22] Chen, H., Teng, Z., Guo, Z., and Zhao, P., 2020, "An Integrated Target Acquisition Approach and Graphical User Interface Tool for Parallel Manipulator Assembly," ASME J. Comput. Inf. Sci. Eng., **20**(2), p. 021006.
[23] Peng, L., and Liu, J., 2018, "Detection and Analysis of Large-Scale wt Blade Surface Cracks Based on Uav-Taken Images," IET Image Process., **12**(11), pp. 2059–2064.
[24] Gong, S., Li, G., Zhang, Y., Li, C., and Yu, L., 2019, "Application of Static Gesture Segmentation Based on an Improved Canny Operator," J. Eng., **2019**(15), pp. 543–546.
[25] Zhang, D., and Lu, G., 2003, "A Comparative Study of Curvature Scale Space and Fourier Descriptors for Shape-Based Image Retrieval," J. Visual Commun. Image Representation, **14**(1), pp. 39–57.